

ASL-incorporated Pharmacokinetic Modelling of PET Data With Reduced Acquisition Time: Application to Amyloid Imaging

Catherine J. Scott¹(✉), Jieqing Jiao¹, Andrew Melbourne¹,
Jonathan M. Schott², Brian F. Hutton^{3,4}, and Sébastien Ourselin^{1,2}

¹ Translational Imaging Group, CMIC, University College London, London, UK
catherine.scott.14@ucl.ac.uk

² Dementia Research Centre, Institute of Neurology,
University College London, London, UK

³ Institute of Nuclear Medicine, University College London, London, UK

⁴ Centre for Medical Radiation Physics, University of Wollongong,
Wollongong, NSW, Australia

Abstract. Pharmacokinetic analysis of Positron Emission Tomography (PET) data typically requires at least one hour of image acquisition, which poses a great disadvantage in clinical practice. In this work, we propose a novel approach for pharmacokinetic modelling with significantly reduced PET acquisition time, by incorporating the blood flow information from simultaneously acquired arterial spin labelling (ASL) magnetic resonance imaging (MRI). A relationship is established between blood flow, measured by ASL, and the transfer rate constant from plasma to tissue of the PET tracer, leading to modified PET kinetic models with ASL-derived flow information. Evaluation on clinical amyloid imaging data from an Alzheimer's disease (AD) study shows that the proposed approach with the simplified reference tissue model can achieve amyloid burden estimation from 30 min [¹⁸F]florbetapir PET data and 5 min simultaneous ASL MR data, which is comparable with the estimation from 60 min PET data (mean error = -0.03). Conversely, standardised uptake value ratio (SUVR), the alternative measure from the data showed a positive bias in areas of higher amyloid burden (mean error = 0.07).

1 Introduction

Position Emission Tomography (PET) is currently the most sensitive *in vivo* molecular imaging technique to provide a non-invasive assay of the human body. Dynamic PET image data acquired following the injection of a radioactive tracer allows the use of pharmacokinetic modelling techniques to quantify a range of biological, physiological and biochemical parameters. However, a typical dynamic PET scan requires at least 1 h to sufficiently cover the underlying processes. The long scan duration is prohibitive for routine clinical use, where time is limited, and data integrity is risked by the increased chance of subject motion.

Currently clinical imaging in PET is often performed using single time point estimates (static imaging) of tracer uptake, such as the standardised uptake value ratio (SUVR). SUVR, a semi-quantitative measure of uptake, is the ratio of the activity concentration within a region relative to the concentration in a tissue which is free from the imaging target, called the reference region. It usually requires 10 min of PET data, which are acquired once non-specifically bound tracer reaches equilibrium between a region and the reference tissue, approximately 50 min or more post injection. This measure is expected to correlate with fully quantitative estimates derived from the full dynamic PET data. However, changes in blood flow affect the delivery of the tracer to tissue and consequently alter the tracer concentration in the tissue when a static image is acquired. Without the blood flow information contained in the early dynamic data, there is no way to account for the influence of the changes in blood flow, thus SUVR values can be biased. This has been highlighted in longitudinal studies, where pathophysiological changes in blood flow have caused spurious changes in SUVR values which do not reflect imaging target abundance [1]. The estimates derived by kinetic modelling are not biased in this way, as the full dynamic curve contains blood flow information, which is parametrised within the model.

In neuroimaging, cerebral blood flow can be measured using arterial spin labelled (ASL) MRI, where magnetically tagged blood is used as an endogenous contrast agent. With the advent of PET-MRI scanners, this information can be acquired concurrently with PET data. Therefore the blood flow information from the ASL can be used in pharmacokinetic analysis when the early part of a dynamic PET scan, which involves blood flow, is not collected. This will lead to the reduction of PET acquisition time needed to perform pharmacokinetic modelling.

In this work, we propose a novel approach for combining PET and ASL information to derive the parameters of interest with a greatly reduced scanning time, Fig. 1. To our knowledge, this is the first time that ASL blood flow estimates have been used to perform PET kinetic analysis to reduce image acquisition time. We evaluated the proposed approach in an AD study using $[^{18}\text{F}]$ florbetapir, a PET radiotracer that binds to amyloid- β , which is considered to be an important target in the AD brain.

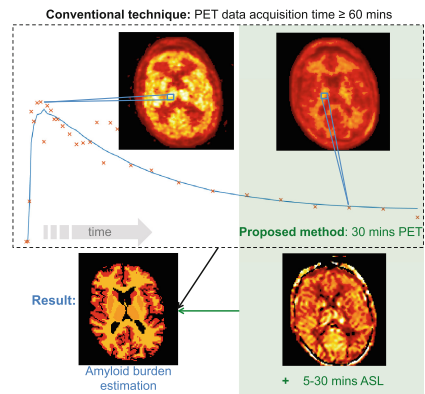


Fig. 1. Dynamic PET acquisition for amyloid burden quantification and time reduction for the proposed method.

2 Methods

2.1 CBF Estimation with ASL MRI

The cerebral blood flow (CBF) map is estimated from pseudo continuous arterial spin labelling (PCASL) data using the relationship established in [2]. The parameter values used in this work were 0.9 ml/g for the plasma/tissue partition coefficient, a blood $T1$ value of 1650 ms, and a labelling efficiency of 0.85.

2.2 Amyloid- β Burden Estimation with SRTM

In this work, the simplified reference tissue model (SRTM) [3] was used to quantify the PET data. SRTM describes the tracer-target interaction using a single tissue compartment model. Using the tracer time activity curve in the reference region $C_R(t)$ as an input function, the operational equation between the tracer time activity curve in the target tissue $C_T(t)$ and $C_R(t)$ is formulated as:

$$C_T(t) = R_1 C_R(t) + \left(k_2 - R_1 \frac{k_2}{1 + BP_{ND}} \right) C_R(t) \otimes e^{-\frac{k_2}{1 + BP_{ND}} t}, \quad (1)$$

where t denotes time and $t = 0$ at tracer injection, R_1 is the local rate of delivery in the target tissue relative to reference tissue, k_2 is the rate constant from target tissue to blood, BP_{ND} is the binding potential that is proportional to the density of amyloid- β , and \otimes denotes the convolution operator. Cerebellar grey matter is used as the reference region to derive $C_R(t)$ as it is considered to be devoid of amyloid- β in this study [4]. BP_{ND} , as the outcome measure of interest to represent the amyloid- β burden, can then be estimated together with R_1 and k_2 by performing curve-fitting using (1) with $C_T(t)$ and $C_R(t)$ extracted from PET data acquired from tracer injection over a sufficient duration. We used a linearised version of SRTM [5] to calculate BP_{ND} , R_1 and k_2 from dynamic PET data of 0:60 min as the gold standard.

2.3 SRTM with Incomplete PET Scan and CBF

Population-Based Extrapolation of Reference Input $C_R(t)$. To estimate BP_{ND} using the PET data where the early part from the tracer injection is absent ($t \in [t_s, t_e]$, $t_s > 0$), firstly extrapolation is required to have the reference input $C_R(t)$ for $t \in [0, t_s]$ so that the convolution term in (1) can be calculated. In this work the whole reference input $C_R(t)$ for $t \in [0, t_e]$ was generated using a single tissue compartment model $C_R(t) = K'_1 e^{-k'_2 t} \otimes \alpha AIF(t)$. If we assume $AIF(t)$, $t \in [0, t_e]$ is a population arterial input function with α being an individual scaling factor, k'_2 a population rate constant from reference tissue to blood, and K'_1 an individual rate constant from blood to reference tissue, then $K'_1 \alpha$ can be estimated by scaling a measured population-based reference input curve $C_R^p(t)$, $t \in [0, t_e]$ to match the individual $C_R(t)$, $t \in [t_s, t_e]$ to generate $C_R(t)$, $t \in [0, t_e]$.

R_1 Estimation with CBF. ASL is used to measure the CBF, flow denoted by F , which is converted into a pseudo R_1 estimate to use in SRTM. R_1 is defined as $R_1 = K_1/K'_1$ where K_1 is the rate constant from blood to target tissue and K'_1 is the rate constant from blood to reference tissue.

Based on the Renkin-Crone model, the relationship between K_1 and F can be described as

$$K_1 = EF = \left(1 - e^{-\frac{PS}{F}}\right) F, \quad (2)$$

where E denotes the net extraction, P is the vessel permeability and S the surface area. Under common physiological conditions of flow, where PS is high ($> 3 \text{ ml} \cdot 100 \text{ g}^{-1} \cdot \text{min}^{-1}$), the relationship between K_1 and flow F is linear. In the absence of knowledge on PS across the brain, we assume that it is sufficiently high such that the relationship between K_1 and F , and in turn the relationship between R_1 and F , can be approximated as a linear function. Linear regression between R_1 and F was performed on a group of subjects, and the linear relationship was then applied to a different group of subjects to convert CBF to a pseudo R_1 value for estimating BP_{ND} with incomplete PET data.

SRTM with CBF-derived R_1 and Extrapolated $C_{R(t)}$. Rewrite (1) as $C'_T(t) = \phi C_R(t) \otimes e^{-\theta t}$, where $C'_T(t) = C_T(t) - R_1 C_R(t)$ is calculated from the $C_T(t)$ and $C_R(t)$ extracted from the measured PET data for $t \in [t_s, t_e]$, and R_1 is derived from the CBF. Here, $\phi = k_2 - R_1 k_2 / (1 + BP_{ND})$ and $\theta = k_2 / (1 + BP_{ND})$ are unknown. To solve ϕ and θ , we used the basis functions defined in [5] to pre-calculate the convolution term using the extrapolated $C_R(t)$, $t \in [0, t_e]$ with a range of biologically plausible values for θ . BP_{ND} and k_2 are then derived from ϕ , θ and the CBF-derived R_1 .

3 Experiments and Results

Data. We evaluated the proposed method on data from 11 cognitively normal subjects participating in Insight 46, a neuroimaging sub-study of the MRC National Survey of Health and Development, who underwent amyloid PET and multi-modal MR imaging on a Siemens Biograph mMR PET/MR scanner. List mode PET data were acquired for 60 min following intravenous injection of [^{18}F]florbetapir, a radiotracer that binds to amyloid- β . For PET image reconstruction, simultaneously acquired structural MR was used to synthesise CT data and calculate the μ -map [6]. Dynamic PET data were binned into $15 \text{ s} \times 4$, $30 \text{ s} \times 8$, $60 \text{ s} \times 9$, $180 \text{ s} \times 2$, $300 \text{ s} \times 8$ time frames, and reconstructed using the manufacturer's software with corrections for dead-time, attenuation, scatter (based on the synthesised CT), randoms and normalisation. PCASL data were acquired using a 3D GRASE readout with voxels of $1.88 \times 1.88 \times 4 \text{ mm}$. 10 control-label pairs were acquired with a pulse duration and post labelling delay of 1800 ms.

Data Processing Framework. T1-weighted images were parcellated [7] into amygdala, pons, brainstem, cerebellum (white and grey separately), hippocampus, cerebral white matter, putamen, thalamus and 6 cortical grey matter

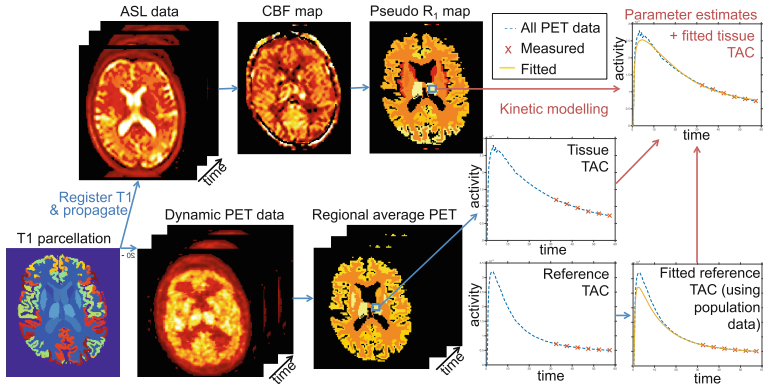


Fig. 2. Overview- parcellation is registered to PET and ASL to calculate regional average values. ASL data is converted into CBF-derived R_1 values using the linear regression relationship. A population reference tissue time activity curve of 0:60 min combined with the measured reference tissue data (30:60 min) is used with the CBF-derived R_1 and the measured PET tissue data (30:60 min), to apply the modified simplified reference tissue model to estimate BP_{ND} .

regions, with left and right hemispheres combined. The T1-weighted image was rigidly registered to both ASL and PET space, and the transformation was propagated to the parcellation. Regional average CBF values were calculated, and the PET time activity curves were averaged across the region prior to kinetic modelling. PET data acquired during 30:60 min were used to evaluate the proposed method. To estimate the reference region activity in the missing time frames, a population averaged reference input was extracted from 14 age matched subjects with 60 min ^{18}F florbetapir PET data. To establish the relationship between the CBF and R_1 values, linear regression was performed on data from 5 subjects and the proposed approach was tested on the remaining 6 subjects. A summary of the data processing framework is shown in Fig. 2.

3.1 Comparison of Proposed Method with Gold Standard

Figure 3a shows BP_{ND} , the measure of the amyloid burden, estimated using the proposed method with 30:60 min data plotted against the gold standard using the full 60 min dynamic data. Linear regression of all subjects and regions shows that the proposed method offers a good approximation of the gold standard as it closely follows the line of identity (blue dashed line), which is within the 95 % confidence interval (CI) of the regression (shaded area). Furthermore, subject specific Pearson correlation coefficients, ρ , show a high linear correlation.

The alternative measure used in clinical practice, $SUVR - 1$, was calculated from PET data over 50:60 min for comparison, Fig. 3b. Whilst ρ is still high for each subject, a clear bias is shown as $SUVR - 1$ overestimates the binding potential at higher values. The mean error quantifies the bias between the estimates and the gold standard which is 0.0740 for $SUVR - 1$, indicative of the

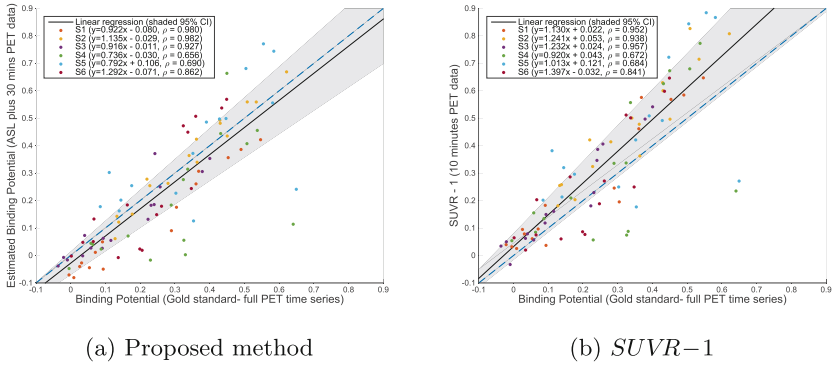


Fig. 3. Estimated amyloid burden against the gold standard value calculated using full PET time series. (Color figure online)

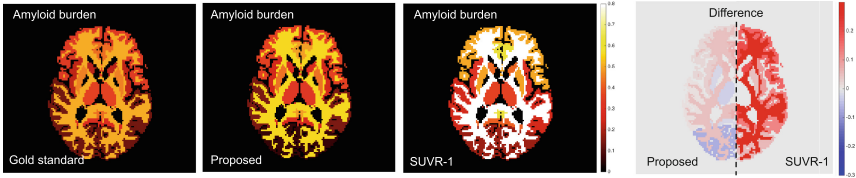


Fig. 4. Regional average binding potential maps for (left to right) gold standard, proposed method, $SUVR-1$, difference maps compared to gold standard.

systematic overestimation, compared to -0.0311 for the proposed method. The proposed method also has a lower mean square error (0.0151 compared to 0.0247 for $SUVR-1$), and variance (0.0142 compared to 0.0194 for $SUVR-1$). Figure 4 shows BP_{ND} maps for a subject, comparing the gold standard with the proposed method and $SUVR-1$ regionally. The proposed method shows good agreement with the gold standard, with slight overestimation of the cortical white matter. For the $SUVR-1$ estimation, amyloid burden is greatly overestimated within both grey and white matter structures. The difference map shows that the errors in the proposed method are far lower than for $SUVR-1$.

3.2 Influence of R_1 Estimation on Amyloid Quantification

Whilst Fig 3a demonstrates a high similarity between binding potential estimation using the gold standard and the proposed method, there is a noise component which introduces variation around the line of identity. This is due to noise in the PET data, noise in the CBF-derived R_1 estimate from the ASL data, and inaccuracies in the estimation of the reference tissue input.

To demonstrate the influence of the CBF-derived R_1 estimate using ASL data, the proposed method was applied using the R_1 estimated using the gold standard technique instead of the CBF-derived R_1 . The population input function and 30:60 min PET data were used as before. This represents the optimal

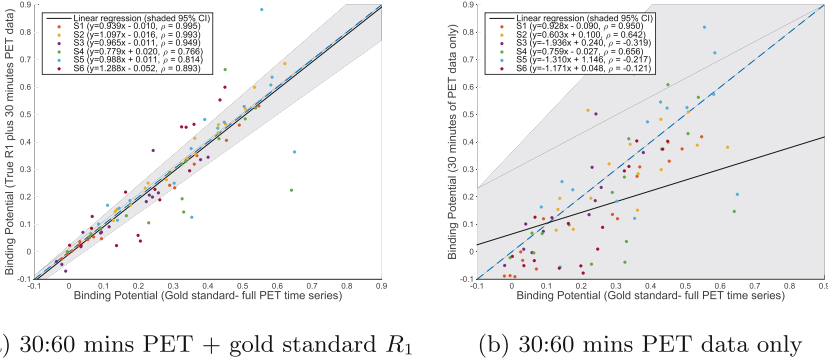


Fig. 5. Estimated binding potential plotted against the gold standard value calculated using full PET time series

case in which R_1 can be determined exactly from the ASL data. Figure 5a shows that the variance in the binding potential estimate has been reduced (from 0.0142 to 0.008), and the linear regression line lies along identity with a narrow CI. This is expected since the CBF map from the ASL is noisy, and linear regression performed to determine the relationship between CBF and R_1 was performed with only 5 subjects, and therefore may not be generalisable. However, for the data used in this study the estimation of R_1 from CBF is sufficiently accurate that the BP_{ND} estimates between the proposed method using CBF-derived R_1 and gold standard R_1 are comparable and there is a reduced bias in the estimates.

Figure 5b compares BP_{ND} estimation using 30:60 min PET data only to the gold standard to demonstrate the need of a CBF-derived R_1 . Due to the lack of data to support the kinetic modelling, the results are noisy and extreme parameter estimates occurred for some regions. These points are beyond the display range in Fig. 5b and have skewed the linear regression such that it no longer follows the identity line, and the 95% CI extends beyond that shown.

4 Discussion and Conclusion

This work demonstrates that the proposed method produces estimates of amyloid burden which are comparable to full pharmacokinetic modelling of 0:60 min [^{18}F]florbetapir PET data, using just 30:60 min of PET data together with blood flow information from ASL. The proposed method is more accurate than the simplified estimate of amyloid burden, $SUVR - 1$, which showed a positive bias especially at higher binding potential values. The results of the proposed technique depend on the CBF-derived R_1 estimate from the ASL data. The ASL data used here were acquired for only 5 min without motion correction, and thus susceptible to artefacts and noise. Linear regression between CBF and R_1 using just 5 subjects could produce errors which may propagate to the binding potential estimation. To reduce the influence of errors in the CBF maps on the

parameter estimation, a more complex kinetic model will be explored in future work to penalise the deviation of R_1 estimation from the CBF-derived R_1 value. The relationship between CBF from ASL and PET R_1 will be further explored to tune this regularisation scheme. The application of this technique to PET tracers which bind to other biological targets of interest will also be explored.

Acknowledgments. This work was supported by the EPSRC UCL Centre for Doctoral Training in Medical Imaging (EP/L016478/1), UCL Leonard Wolfson Experimental Neurology Centre (PR/ylr/18575), EPSRC (EP/H046410/1, EP/J020990/1, EP/K005278), MRC (MR/J01107X/1), NIHR UCLH Biomedical Research Centre (inc. High Impact Initiative, BW.mn.BRC10269). Insight 1946 receives funding from Alzheimer’s Research UK (ARUK-PG2014-1946), MRC Dementia Platform UK (CSUB19166) and The Wolfson Foundation, and support from Avid Radiopharmaceuticals, a wholly owned subsidiary of Eli Lilly. We are grateful to the Insight 46 participants for their involvement in this study.

References

1. Cselényi, Z., Farde, L.: Quantification of blood flow-dependent component in estimates of beta-amyloid load obtained using quasi-steady-state standardized uptake value ratio. *J. Cereb. Blood Flow Metab.* **35**, 1–9 (2015)
2. Melbourne, A., Toussaint, N., Owen, D., Simpson, I., Anthopoulos, T., De Vita, E., Atkinson, D., Ourselin, S.: Niftyfit: a software package for multi-parametric model-fitting of 4D magnetic resonance imaging data. *Neuroinformatics* **14**(3), 319–337 (2016)
3. Lammertsma, A., Hume, S.: Simplified reference tissue model for PET receptor studies. *Neuroimage* **158**(4), 153–158 (1996)
4. Klunk, W.E., Engler, H., Nordberg, A., Wang, Y., Blomqvist, G., Holt, D.P., Bergström, M., Savitcheva, I., Huang, G.F., Estrada, S., Ausén, B., Debnath, M.L., Barletta, J., Price, J.C., Sandell, J., Lopresti, B.J., Wall, A., Koivisto, P., Antoni, G., Mathis, C., Långström, B.: Imaging brain Amyloid in Alzheimer’s disease with pittsburgh compound-B. *Ann. Neurol.* **55**(3), 306–319 (2004)
5. Gunn, R.N., Lammertsma, A.A., Hume, S.P., Cunningham, V.J.: Parametric imaging of ligand-receptor binding in PET using a simplified reference region model. *NeuroImage* **6**(4), 279–287 (1997)
6. Burgos, N., Cardoso, M.J., Thielemans, K., Modat, M., Dickson, J., Schott, J.M., Atkinson, D., Arridge, S.R., Hutton, B.F., Ourselin, S.: Multi-contrast attenuation map synthesis for PET/MR scanners: assessment on FDG and florbetapir PET tracers. *Eur. J. Nucl. Med. Mol. Imaging* **42**(9), 1447–1458 (2015)
7. Cardoso, M.J., Modat, M., Wolz, R., Melbourne, A., Cash, D., Rueckert, D., Ourselin, S.: Geodesic information flows: spatially-variant graphs and their application to segmentation and fusion. *IEEE TMI* **99**, 1976–1988 (2015)